Multi-fluid models for two-phase and transcritical flows Application to rocket engine configurations with the AVBP solver

Thomas Schmitt, Milan Pelletier, Sébastien Ducruix

Noname manuscript No.
(will be inserted by the editor)

Multi-fluid models for two-phase and transcritical flows

Application to rocket engine configurations with the AVBP solver

Thomas Schmitt, Milan Pelletier and Sébastien Ducruix

the date of receipt and acceptance should be inserted later

Abstract In various industrial combustion devices, such as liquid rocket engines or Diesel engines, the operating point varies over a wide range of pressure. These pressure variations can lead to a change of thermodynamic regime, switching from two-phase injection to transcritical injection. This change may modify the topology of the flow and the mixing, thereby impacting the flame dynamics. In the present contribution, a framework that is able to simulate compressible flows under both subcritical and supercritical states within the same solver is presented. This is achieved using a multifluid approach coupled with a cubic equation of state (EoS). Liquid/vapor equilibrium is computed within the binodal region to ensure the convexity of the EoS. Examples of coaxial flame simulations are provided, showing good agreements with experimental visualizations.

Keywords Two-phase flow · Supercritical flow · Non-Ideal thermodynamics · Large-Eddy Simulation

1 Introduction

The jet formed during liquid injection is strongly dependent on the operating temperature and pressure conditions. When pressure and temperature are low enough with respect to the critical point, the fluid undergoes a classical break-up process. The interfaces correspond to discontinuities between the liquid and gas phases. As pressure or temperature are increased to supercritical conditions, surface tension vanishes and the phase discontinuity that is observed at lower pressure is no longer present. Instead, the jet evolves in the presence of a continuous interface between the high-density stream and the surrounding gases. Thermodynamic properties feature strong - but continuous - variations across a diffuse interface. Under such conditions, the fluid injection regime is often referred to as transcritical and the jet mixing is controlled by turbulence and is analogous to that of a variable density jet [2].

Supercritical and transcritical injection modeling has been deeply investigated during the last decades [11,20]. One important ingredient of such models is the appropriate description of the real-gas thermodynamics that drives the fluid behavior in such high pressure / low temperature situations. Thermodynamics generally rely on the use of a cubic equation of state, such as the Soave Redlich Kwong EoS [17]. In the context of Large-Eddy Simulations, good results have been obtained for the simulation of cryogenic coaxial flames, with satisfactory agreements in terms of flame topology between simulations and experiments [19,15].

For compressible cases, the strategies encountered in the literature for the modeling of separate two-phase flows mostly focus on diffuse interface methods and more specifically on multi-fluid methods [1,14]. These methods seem well-adapted by construction to handle the interface appearance and disappearance that may occur in the targeted applications. They rely on an ensemble

Laboratoire EM2C, CNRS, CentraleSupélec, Université Paris-Saclay,
3, rue Joliot Curie, 91192 Gif-sur-Yvette cedex, France
Tel.: +33 1 75 31 60 91
E-mail: thomas.schmitt@centralesupelec.fr, thomas.schmitt@cnrs.fr

averaging of the phases properties to formulate sets of equations that rule the two-phase flow evolution, which are hyperbolic provided that convex thermodynamic closures are used [14]. Under the assumption of pressure, temperature and chemical potentials equilibria between phases, simplified multifluid models can be derived, convenient to treat numerically [7]. Such models have been recently coupled with cubic EoS and a multicomponent two-phase equilibrium solver in a classic finite-volume framework [9,18], showing very good results with available experimental data in the context of turbulent multi-component jet injection.

In the present contribution, a multi-fluid approach is combined with a cubic equation of state in the finite-element LES solver AVBP [16,15,8] to simulate coaxial cryogenic flames operating at sub- and supercritical pressure. The governing equations and models are detailed in Sec. 2 and the thermodynamic closure is given in Sec. 3. Finally, examples of coaxial flame simulations are provided in Sec. 4.

2 Governing equations

Both 3- and 4-equation models have been integrated in the AVBP solver (see [8] for details). The three equation model, used in the simulations presented below, is detailed in this section. This model being similar to Euler equations used in gaseous and supercritical flows, similar closure are used here [15]. In the context of Large-Eddy Simulation, the corresponding Favre-filtered, fully compressible Navier-Stokes equations are given by:

$$\frac{\partial \overline{\rho}\widetilde{Y_k}}{\partial t} + \frac{\partial \overline{\rho}\widetilde{Y_k}\widetilde{u}_j}{\partial x_j} = -\frac{\partial \overline{J_{k,j}}}{\partial x_j} - \frac{\partial J^t_{k,j}}{\partial x_j} + \overline{\dot{\omega}_k} \tag{1}$$

$$\frac{\partial \overline{\rho}\widetilde{u}_i}{\partial t} + \frac{\partial \overline{\rho}\widetilde{u}_i\widetilde{u}_j}{\partial x_j} = -\frac{\partial \overline{p}}{\partial x_i} + \frac{\partial \overline{\tau_{i,j}}}{\partial x_j} + \frac{\partial \tau^t_{i,j}}{\partial x_j} \tag{2}$$

$$\frac{\partial \overline{\rho}\widetilde{E}}{\partial t} + \frac{\partial \overline{\rho}\widetilde{u}_j\widetilde{E}}{\partial x_j} = -\frac{\partial \overline{p}\widetilde{u}_j}{\partial x_j} + \frac{\partial \widetilde{u}_i\overline{\tau_{i,j}}}{\partial x_j} - \frac{\partial \overline{q_j}}{\partial x_j} - \frac{\partial q^t_j}{\partial x_j} + \overline{\dot{\omega}_T} \tag{3}$$

where $\overline{\phi}$ and $\tilde{\phi}$ denote spatial and mass-weighted (Favre) spatially filtered quantities. p is the pressure, T the temperature, ρ the density, Y_k is the mass fraction of the species k, u_i represents the velocity vector components, x_i the spatial coordinates, t is the time, E the total sensible energy, $\tau^t_{i,j}$ the sub-grid scale (SGS) stress tensor, q^t_j the SGS energy fluxes, $J^t_{k,j}$ the SGS species fluxes, $\dot{\omega}_k$ the species reaction rate and $\dot{\omega}_T$ the heat release rate. The species $\mathbf{J}_k$ and heat fluxes $\mathbf{q}$ use classical gradient approaches. The fluid viscosity and the heat diffusion coefficient are calculated following Chung *et al.* method [3] and mass diffusion coefficients are deduced from heat diffusivity by assuming a unity Lewis number (Le=1). Soret and Dufour effects are neglected. The sub-grid scale (SGS) energy and species fluxes are modeled using the gradient transport assumption with turbulent Prandtl and Schmidt numbers both set to 0.7. The SGS turbulent viscosity is modeled with the *wall-adapting large eddy* (WALE) model [10]. In the present work, combustion is modeled assuming infinitely fast reactions and pure diffusion regime operation [15].

3 Thermodynamic closure

Mixture properties are computed using the Soave-Redlich-Kwong (SRK) EoS [17]:

$$p(\rho, T, Y) = \frac{\rho r T}{1 - b_m \rho} - \frac{a_m(T)\rho^2}{1 - b_m^2 \rho^2} \tag{4}$$

with the mixture covolume b_m and attractive coefficient a_m computed following the van der Waals mixing laws [13]. In the subcritical domain, single-phase states can become unstable, leading to phase separation. The instability can be mechanical or chemical in the case of multicomponent mixtures, corresponding respectively to a loss of thermodynamic convexity along the pressure direction or along the chemical composition directions. Convexity can be restored by computing an equilibrium between a liquid and a vapor phase. In the present contribution, an approximation of the exact multi-component equilibrium is used assuming that, for each species, the liquid and vapor

phase mass fractions are equal. Such an approximation is reasonable as long as phase separation is not dominated by a chemical instability. Practical methods for its calculation as well as more elaborated equilibrium closures are detailed in [8,12].

4 Application to the Mascotte test-cases

4.1 Simulated cases and numerical setup

The Mascotte experimental configuration of ONERA is considered here [5,2]. The present simulations reproduce cases A10 and C10 [6]. Simulation of cases operating at 60 bar (i.e. under transcritical conditions) can be found in [15]. A single coaxial injector produces a liquid oxygen stream at low velocity (less than 10 m/s), surrounded by a high-velocity gaseous hydrogen stream (more than 100 m/s), in a chamber at 10 bar. Liquid oxygen is injected at 80 K, well below its critical value of 155 K, while gaseous hydrogen is injected at 289 K. Under such conditions, the density of oxygen ($\rho_{O_2} = 1190$ kg.m^{-3}) is much larger than that of hydrogen ($\rho_{H_2} = 0.85$ kg.m^{-3}). Injection conditions are summarized in Tab. 4.1

Table 1 Injection conditions for the simulated cases. $\dot{m}$ is the mass flow rate, Tr=T/Tc is the reduced temperature and Pr=p/pc is the reduced pressure, Tc and Pc being the critical temperature and pressure, respectively.

Case	Pressure [bar]	$\dot{m}_{H_2}$ [g/s]	$\dot{m}_{O_2}$ [g/s]	Tr_{O_2}	Pr_{O_2}
A10	10.0	23.7	50	0.52	0.20
C10	10.0	15.8	50	0.52	0.20

The compressible unstructured solver AVBP [16] is used for this study. Its Taylor-Galerkin weighted residual central distribution scheme, called TTGC, is third-order in time and space [4]. The Jacobian matrices of non-viscous fluxes used by the scheme and the characteristic boundary conditions are written to be fully consistent with the non-ideal thermodynamics [8].

4.2 Preliminary results

On going simulations results are shown in this section. A longitudinal slice of instantaneous temperature field for case A10 is shown in Fig. 1. A fully turbulent diffusion flame emanates from the coaxial injector. The white iso-contour shows the regions of liquid/vapor coexistence, which is essentially located after the liquid jet break-up. Simulations are qualitatively compared with experimental results in Fig. 2, where mean OH mass fraction field is compared with OH* emission exprimental pictures from Kendrick et al. [6]. For both cases, the initial open angle is well reproduced and the flame shape is qualitatively retrieved. However, flames seem to be slightly longer in the simulations compared with the experiment.

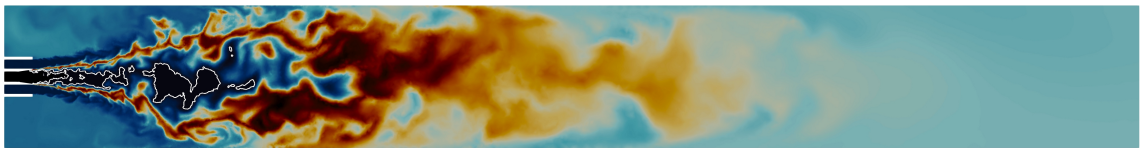

Fig. 1 Longittudinal slice of instantaneous temperature for case A10. Blue: 80 K, Red: 3400 K. The white iso-contour represents liquid/vapor coexistence regions where the mixture is thermodynamically unstable.

5 Conclusion

A 3-equation multifluid model coupled with a cubic equation of state assuming thermodynamical equilibrium in the binodal region is presented in this contribution. The model is integrated in the

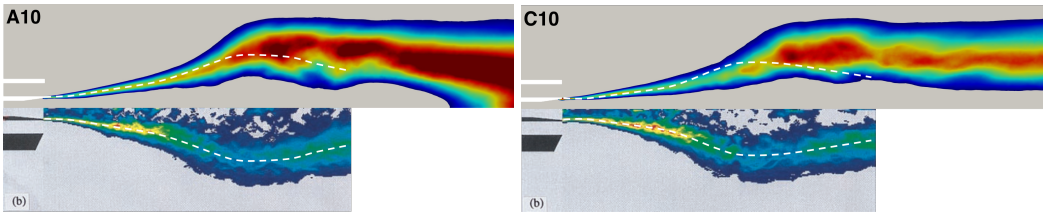

Fig. 2 *Comparison with experimental visualizations.* Comparison between Abel's transform of experimental OH* mean emission for case A10 and C10 [6] (bottom part of the pictures) and a longitudinal cut of mean OH mass fraction (Blue: 0.01, red: 0.05) from LES (top part of the pictures). Dashed lines show the position of maximum OH* emission from experiments. Note that the experimental visualization for case A10 is not perfectly symmetrical, comparison is thus qualitative.

AVBP solver and permits the simulation of subcritical to supercritical cryogenic flames. Results are in satisfactory agreement with experimental visualizations.

Acknowledgements This work was granted access to HPC resources made available by GENCI (Grand Equipement National de Calcul Intensif) under the allocation A0082B06176. A part of this work was performed using HPC resources from the mesocentre computing center of Ecole CentraleSupélec and Ecole Normale Supérieure Paris-Saclay supported by CNRS and Région Ile-de-France.

References

1. Baer, M., Nunziato, J.: A two-phase mixture theory for the deflagration-to-detonation transition (ddt) in reactive granular materials. International journal of multiphase flow **12**(6), 861–889 (1986)
2. Candel, S., Juniper, M., Singla, G., Scouflaire, P., Rolon, C.: Structure and dynamics of cryogenic flames at supercritical pressure. Combustion Science and Technology **178**(1-3), 161–192 (2006)
3. Chung, T.H., Ajlan, M., Lee, L.L., Starling, K.E.: Generalized multiparameter correlation for nonpolar and polar fluid transport properties. Industrial & engineering chemistry research **27**(4), 671–679 (1988)
4. Colin, O., Rudgyard, M.: Development of high-order Taylor–Galerkin schemes for LES. Journal of Computational Physics **162**(2), 338–371 (2000)
5. Habiballah, M., Orain, M., Grisch, F., Vingert, L., Gicquel, P.: Experimental studies of high-pressure cryogenic flames on the Mascotte facility. Combustion Science and Technology **178**(1-3), 101–128 (2006)
6. Kendrick, D., Herding, G., Scouflaire, P., Rolon, C., Candel, S.: Effects of a recess on cryogenic flame stabilization. Combustion and Flame **120**(3), 404 – 406 (2000). DOI https://doi.org/10.1016/S0010-2180(99)00151-0. URL http://www.sciencedirect.com/science/article/pii/S0010218099001510
7. Le Martelot, S., Saurel, R., Nkonga, B.: Towards the direct numerical simulation of nucleate boiling flows. International Journal of Multiphase Flow **66**, 62–78 (2014)
8. M. Pelletier, T.S., Ducruix, S.: A multifluid taylor-galerkin methodology for the simulation of compressible multicomponent separate two-phase flows from subcritical to supercritical states. Computers & Fluids **206**(104588) (2020)
9. Matheis, J., Hickel, S.: Multi-component vapor-liquid equilibrium model for LES of high-pressure fuel injection and application to ECN spray A. International Journal of Multiphase Flow **99**, 294–311 (2018)
10. Nicoud, F., Ducros, F.: Subgrid-scale stress modelling based on the square of the velocity gradient tensor. Flow, turbulence and Combustion **62**(3), 183–200 (1999)
11. Oefelein, J.C.: Mixing and combustion of cryogenic oxygen-hydrogen shear-coaxial jet flames at supercritical pressure. Combustion Science and Technology **178**(1-3), 229–252 (2006). DOI 10.1080/00102200500325322
12. Pelletier, M.: Diffuse interface models and adapted numerical schemes for the simulation of subcritical to supercritical flows. Ph.D. thesis, Université Paris-Saclay (2019)
13. Poling, B.E., Prausnitz, J.M., John Paul, O., Reid, R.C.: The properties of gases and liquids, vol. 5. Mcgraw-hill New York (2001)
14. Saurel, R., Abgrall, R.: A multiphase Godunov method for compressible multifluid and multiphase flows. Journal of Computational Physics **150**(2), 425–467 (1999)
15. Schmitt, T.: Large-eddy simulations of the Mascotte test cases operating at supercritical pressure. Journal of Flow, Turbulence and Combustion **105**, 159–189 (2020)
16. Schönfeld, T., Rudgyard, M.: Steady and unsteady flows simulations using the hybrid flow solver avbp. AIAA Journal **37**(11), 1378–1385 (1999)
17. Soave, G.: Equilibrium constants from a modified Redlich-Kwong equation of state. Chemical Engineering Science **27**(6), 1197 – 1203 (1972). DOI https://doi.org/10.1016/0009-2509(72)80096-4. URL http://www.sciencedirect.com/science/article/pii/0009250972800964
18. Traxinger, C., Zips, J., Pfitzner, M.: Single-phase instability in non-premixed flames under liquid rocket engine relevant conditions. Journal of Propulsion and Power **35**(4), 675–689 (2019)
19. Zips, J., Müller, H., Pfitzner, M.: Efficient thermo-chemistry tabulation for non-premixed combustion at high-pressure conditions. Flow, Turbulence and Combustion **101**(3), 821–850 (2018)
20. Zong, N., Yang, V.: Cryogenic fluid jets and mixing layers in transcritical and supercritical environments. Combustion science and technology **178**(1-3), 193–227 (2006)